Materials Physics and Mechanics 48 (2022) 44-60
Research article

Received: November 15, 2021
Accepted: November 16, 2021

# ELASTICITY OF THIN DILATATIONAL DISK IN AN ISOTROPIC HALF-SPACE

**T. Nguyen Van[1]✉, A.L. Kolesnikova[2], A.E. Romanov[3]**

[1]Saint-Petersburg, ITMO University, Tchaikovsky str., 11/2, lit. A, Saint-Petersburg, Russia, 191187

[2]Institute for Problems of Mechanical Engineering RAS, 61, Bolshoi Pr. V.O., St. Petersburg, Russian Federation, 199178

[3]ITMO University, 49, Kronverkskiy Pr., St. Petersburg, Russia

✉ nguyenvantuyendhsd@gmail.com

**Abstract.** In this article, the solution to the elasticity boundary-value problem for an infinitesimally thin dilatational disk (ITDD) embedded in an elastically isotropic half-space is presented. The plane of the disk is parallel to the free surface. To solve the boundary value problem, the method of virtual defects is used. The image (mirror) ITDD and radial Somigliana dislocation loops (RSDLs), distributed continuously over the free surface coaxially with the ITDD, are chosen as virtual defects. The ITDD displacements, strains, and stresses are represented in the form of the sums of the Lipschitz-Hankel integrals. It is shown that the elastic field of the ITDD disk is distorted near the free surface and possesses nonzero dilatation and hydrostatic stress. Numerical estimates of dilatation are given and its influence on some characteristics of semiconductors is briefly discussed.
**Keywords:** dilatational disk, isotropic elasticity, half-space, elastic fields

***Acknowledgements***. *Authors thank Russian Science Foundation for the support under project* # 19-19-00617.

**Citation:** Nguyen Van T., Kolesnikova A.L., Romanov A.E. Elasticity of thin dilatational disk in an isotropic half-space // Materials Physics and Mechanics. 2022, V. 48. N. 1. P. 44-60. DOI: 10.18149/MPM.4812022_5.

## 1. Introduction

The role of stressors – sources of internal mechanical stresses and elastic strains in unloaded solids can be hardly overestimated. They can affect practically all physical and mechanical properties of solids. First, the stored elastic energy associated with stressors can be released giving rise to the formation of various defects such as dislocations, cracks, etc. [1-4]. Second, stressors induce elastic distortions changing interatomic distances from their equilibrium values and thus changing materials properties [5-8]. For example, in semiconductors, elastic strains (and stressors as one of the reasons for them) modify the lattice constant and symmetry [9] and therefore control electronic band structure that has a significant effect on the electronic, piezoelectric, and optical properties of semiconductor materials. Examples of the studies of such effects in various semiconductors can be found in Refs. [10,11].

In general, stressors can be considered as singularities of the elastic continuum with a particular geometry of the domain for their localization. This means that there are point (0D), linear (1D), surface (2D), and volume (3D) stressors. One might note that such a

http://dx.doi.org/10.18149/MPM.4812022_5

consideration of stressors is related to the classification of defects in crystals and solids [12,13]. Therefore, stressors are nothing else as well-known defects: point defects, dislocations and disclinations, planar defects, and elastic inclusions. We have also to note that cracks and inhomogeneities and other stress concentrators are excluded from the class of stressors because they generated no elastic field in the absence of external load.

In this study, we focus on a stressor with circular geometry – a thin dilatational disk-like inclusion placed in the vicinity of the free surface of an elastically isotropic half-space. Investigation of such type of a stressor is dictated by the important results for point center of dilatation and ellipsoidal inclusion [10] that evidenced a strong screening of elastic fields of the stressors by a free surface. In this connection, it is worth mentioning a set of publications devoted to the elasticity problems for circular defects and inclusions interacting with plane-free surface or phase boundaries. Circular loop defects near a free surface or in a plate-free surface have been studied for prismatic dislocation rings in Refs. [14,15]. Elastic fields of quantum dots, cuboidal inclusions, dislocation loops, and spherical inclusions in half-space have been studied in Refs. [15-19].

In Section 2 we start with the statement of the elasticity problem for the infinitesimally thin dilatational disk (ITDD) placed at the finite distance from the surface of an isotropic half-space. In Section 3 we provide the necessary background on the elastic properties of the ITDD in infinite media and give the formulas for elastic fields for the radial Somigliana dislocation loop (RSDL). This will allow us to find the close-form solution for elastic fields of the ITDD in an isotropic half-space in Section 4. Then, we discuss the found results in Section 5 and conclude in Section 6.

## 2. Statement of the problem and the method of solution

As shown in Fig. 1, the stressor - infinitesimally thin dilatational disk of radius $a$ is placed at a distance $d$ from the free surface in the isotropic elastic half-space. This defect is defined by the following eigenstrain [20]:

$$\varepsilon_{ii}^{*} = bH\left(1-\frac{r}{a}\right)\delta(z+d),\ i=r,\varphi,z\,, \tag{1}$$

where $b$ is a dimensional factor characterizing the local magnitude of dilatation; $H(\zeta)=\begin{cases}1, \zeta \geq 0\\ 0, \zeta < 0\end{cases}$ is Heaviside step-function; $\delta(z)$ – Dirac delta-function; $r, \varphi, z$ are cylindrical coordinates (see Fig. 1), and no Einstein summation rule is used.

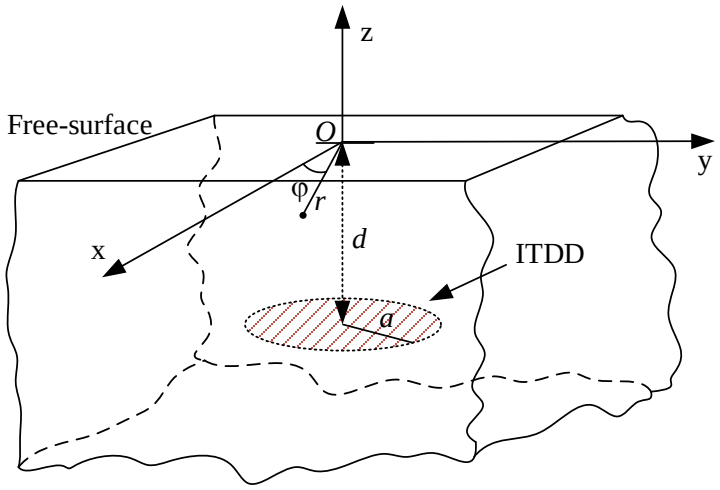


**Fig. 1.** The stressor in the form of the infinitesimally thin dilatational disk (ITDD), near a planar free surface of a half-space

The ITDD is perfectly aligned with the surrounding matrix. The free surface is flat, smooth, and stress-free. The elasticity for the material of a half-space is linear and thus, obeys Hooke's law [21]:

$$\sigma_{ij} = 2G\left( \varepsilon_{ij} + \frac{\nu}{1-2\nu}\varepsilon_{kk}\delta_{ij} \right), i,\ j,\ k = \begin{cases} x,\ y,\ z \\ \text{or} \\ r,\ \varphi,\ z \end{cases}, \tag{2}$$

where Cartesian $x, y, z$ or cylindrical $r, \varphi, z$ coordinates can be used; $\sigma_{ij}$ and $\varepsilon_{ij}$ are components of stress and elastic strain tensors, respectively; $G$ is the modulus of elasticity in shear and $\nu$ is Poisson's ratio, $\delta_{ij}$ is Kronecker delta; and Einstein summation rule is applied.

The boundary conditions at the load-free surface can be written in the following form:

$$\sigma_{iz}^{\text{hs}}\Big|_{z=0} = 0, i = \begin{cases} x,\ y,\ z \\ \text{or} \\ r,\ \varphi,\ z \end{cases}, \tag{3}$$

where $\sigma_{ij}^{\text{hs}}$ are the stresses of the defect placed in the elastic half-space that should be found as a result of the solution of the elasticity boundary-value problem.

The solution of such types of elasticity problems can be reached by exploring the virtual defect method known in the theory of defects. In this method, the elastic field $p_{ij}$ (displacements, strains, and stresses) of the real defect is represented as [22,23]

$$p_{ij} = {}^{\infty}p_{ij} + {}^{\text{i}}p_{ij}, \tag{4}$$

where ${}^{\infty}p_{ij}$ is the field of real defect under consideration in an infinite medium without free surface or interfaces, ${}^{\text{i}}p_{ij}$ is the additional field due to ensembles of virtual defects distributed with distribution functions ${}^{k}f(\xi)$ (where index $k$ is a counter for virtual defect ensembles and $\xi$ is a variable characterizing the position of a probe virtual defect in the ensemble) and placed in an infinite elastic medium. For planar boundaries, ensembles of virtual defects are placed either on free surfaces or at some distance from the interfaces [24-26]. In degenerate cases, instead of distributions one can have isolated defects, which are known as image or mirror defects [22].

Boundary conditions at free faces and/or interfaces dictate the value of the elastic field there:

$$p_{ij}\Big|_S = \alpha_{ij}, \tag{5}$$

where $\alpha_{ij}$ are well-defined functions depending on the radius vector pointing to the points of the surface and/or interface. By using the form for elastic field from Eq. (4) in the boundary conditions of Eq. (5), one can arrive in the equations for unknown distribution functions ${}^{k}f(c)$ of virtual defects. When these functions are found the solution of the boundary-value problem for the defect acquires the following form:

$$p_{ij} = {}^{\infty}p_{ij}\Big|_S + \sum_k \int_D {}^{k}f(\xi)\,{}^{k}p_{ij}\Big|_S\, d\xi, \tag{6}$$

where the integration is performed over the domain D of the virtual defect distribution.

In this work, we consider the combination of continuously distributed virtual defects placed directly on the free surface with the single image defect. To solve the cylindrical symmetry problem, we choose the radial Somigliana dislocation loops as virtual surface defects and additional infinitesimally thin dilatational disk with opposite sign of dilatation as an image (mirror) defect.

## 3. Background

**Elastic fields of an infinitesimally thin dilatational disk in an infinite elastically isotropic medium.** We reproduce the results of works [13,20,27] for elastic fields of ITDD in an infinite isotropic elastic medium. The elastic fields are given in the coordinate system with the origin in the center of the disk, see Fig. 2.

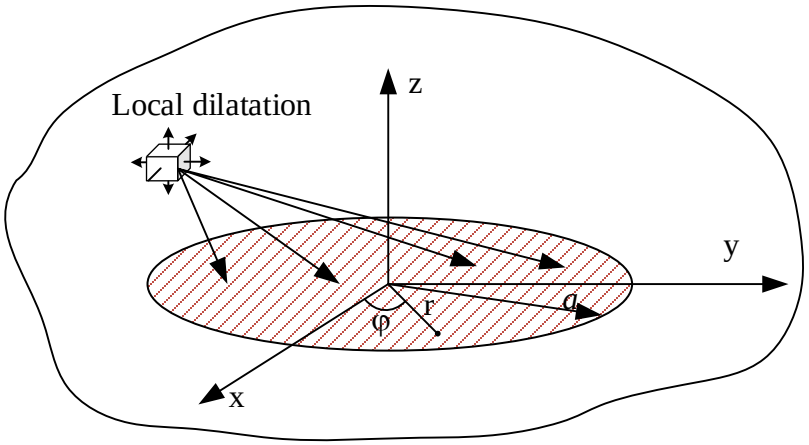


**Fig. 2**. The infinitesimally thin dilatational disk (ITDD) in an infinite isotropic elastic medium

The total displacements $u_i^t$ and total strains $\varepsilon_{ij}^t$ of the ITDD in a continuous medium consist of two parts: elastic $(u_i, \varepsilon_{ij})$ part and related to eigenstrain $(u_i^*, \varepsilon_{ij}^*)$ ones [28]:

$$u_i^{\mathrm{t}} = u_i + u_i^* . \tag{7}$$

$$\varepsilon_{ij}^{\mathrm{t}} = \varepsilon_{ij} + \varepsilon_{ij}^* . \tag{8}$$

The ITDD displacements were found in the following form [13]:

$$u_r^{\mathrm{t}} = \frac{(1+\nu)b}{2(1-\nu)} J(1,1;0), \tag{9a}$$

$$u_\varphi^{\mathrm{t}} = 0, \tag{9b}$$

$$u_z^{\mathrm{t}} = \frac{(1+\nu)}{2(1-\nu)} \mathrm{sgn}(z) J(1,0;0) . \tag{9c}$$

Here $J(m, n; p)$ are the Lipschitz-Hankel integrals:

$$J(m,n;p) = \int_0^{+\infty} J_m(\kappa) J_n\left(\frac{r}{a}\kappa\right) e^{-\frac{|z|}{a}\kappa} d\kappa . \tag{10}$$

where $J_m$ and $J_n$ are Bessel functions of the first kind.

With the help of found displacements elastic strains $\varepsilon_{ij}$ of the ITDD are determined as:

$$\varepsilon_{rr} = \frac{\partial u_r^{\mathrm{t}}}{\partial r} - \varepsilon_{rr}^* = \frac{(1+\nu)b}{2(1-\nu)} \left( \frac{1}{a} J(1,0;1) - \frac{1}{r} J(1,1;0) \right), \tag{11a}$$

$$\varepsilon_{\varphi\varphi} = \frac{u_r^{\mathrm{t}}}{r} - \varepsilon_{\varphi\varphi}^* = \frac{(1+\nu)b}{2(1-\nu)r} J(1,1;0) , \tag{11b}$$

$$\varepsilon_{zz} = \frac{\partial u_z^{\mathrm{t}}}{\partial z} - \varepsilon_{zz}^* = -\frac{(1+\nu)b}{2(1-\nu)a} J(1,0;1) , \tag{11c}$$

$$\varepsilon_{rz} = \frac{1}{2}\left( \frac{\partial u_z^{\mathrm{t}}}{\partial r} + \frac{\partial u_r^{\mathrm{t}}}{\partial z} \right) = -\frac{(1+\nu)b}{2(1-\nu)a} \mathrm{sgn}(z) J(1,1;1) , \tag{11d}$$

$$\varepsilon_{r\varphi} = \varepsilon_{\varphi z} = 0 . \tag{11e}$$

It is easy to check that the trace of the elastic strain tensor (volumetric strain) of the ITDD in an infinite elastically isotropic medium vanishes:

$$\varepsilon = \varepsilon_{ii} = \varepsilon_{rr} + \varepsilon_{\varphi\varphi} + \varepsilon_{zz}$$
$$= \frac{(1+\nu)b}{4(1-\nu)}\left(\frac{2}{a}J(1,0;1) - \frac{2}{r}J(1,1;0)\right) + \frac{(1+\nu)b}{2(1-\nu)r}J(1,1;0) - \frac{(1+\nu)b}{2(1-\nu)a}J(1,0;1) \equiv 0. \qquad (12)$$

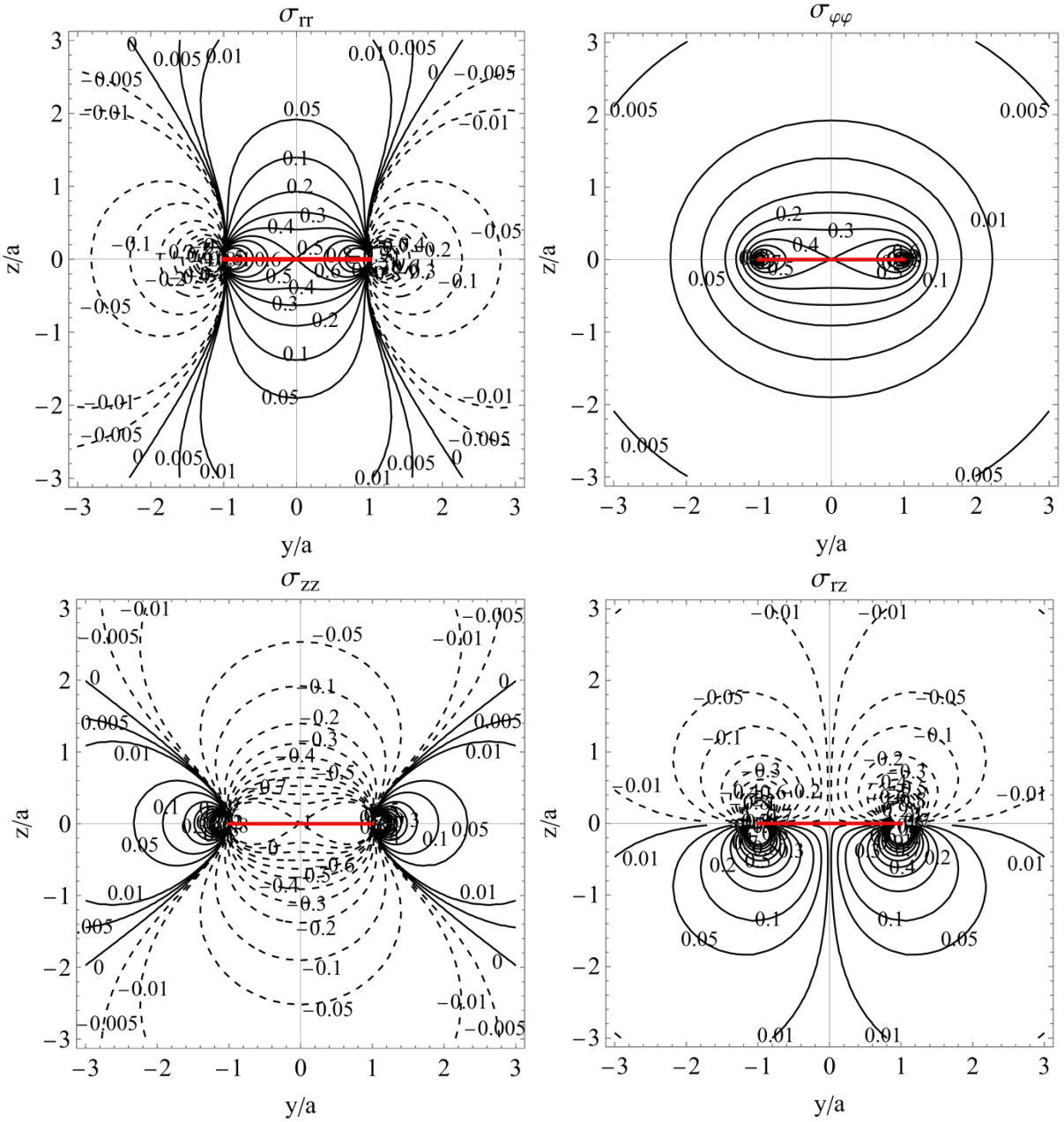


**Fig. 3.** Stress maps in the *zy* - plane for the ITDD, which is in the infinite elastic medium. The stresses are given in units of $G\frac{(1+\nu)b}{(1-\nu)a}$ and the coordinates are normalized to the disk radius *a*

This reduces Hooke's law given by Eqs. (2) to the simpler form $\sigma_{ij} = 2G\varepsilon_{ij}$, which allows finding the stresses of ITDD:

$$\sigma_{rr} = G\frac{(1+\nu)b}{(1-\nu)}\left(\frac{1}{a}J(1,0;1) - \frac{1}{r}J(1,1;0)\right), \qquad (13a)$$

$$\sigma_{\varphi\varphi} = G\frac{(1+\nu)b}{(1-\nu)r}J(1,1;0), \tag{13b}$$

$$\sigma_{zz} = -G\frac{(1+\nu)b}{(1-\nu)a}J(1,0;1), \tag{13c}$$

$$\sigma_{rz} = -G\frac{(1+\nu)b}{(1-\nu)a}\mathrm{sgn}(z)J(1,1;1), \tag{13d}$$

$$\sigma_{r\varphi} = \sigma_{\varphi z} = 0. \tag{13e,f}$$

Obviously, that stresses defined by Eqs. (13) satisfy the equation of equilibrium [21]:

$$\frac{\partial\sigma_{rr}}{\partial r}+\frac{1}{r}\frac{\partial\sigma_{r\varphi}}{\partial\varphi}+\frac{\partial\sigma_{rz}}{\partial z}+\frac{1}{r}\left(\sigma_{rr}-\sigma_{\varphi\varphi}\right)=0, \tag{14a}$$

$$\frac{\partial\sigma_{r\varphi}}{\partial r}+\frac{1}{r}\frac{\partial\sigma_{\varphi\varphi}}{\partial\varphi}+\frac{\partial\sigma_{\varphi z}}{\partial z}+\frac{2}{r}\sigma_{r\varphi}=0, \tag{14b}$$

$$\frac{\partial\sigma_{rz}}{\partial r}+\frac{1}{r}\frac{\partial\sigma_{\varphi z}}{\partial\varphi}+\frac{\partial\sigma_{zz}}{\partial z}+\frac{1}{r}\sigma_{rz}=0. \tag{14c}$$

From Eqs. (13) we easily see that the hydrostatic stress is: $\sigma=\sigma_{rr}+\sigma_{\varphi\varphi}+\sigma_{zz}\equiv 0$. This property that is observed for the stresses of ITDD, is characteristic of all dilatational defects placed in an infinite isotropic medium. The maps of non-zero stress tensor components of ITDD shown in Fig. 2 are given in Fig. 3.

**Elastic fields of a radial Somigliana dislocation loop in an infinite elastically isotropic medium.** In the solution of the elasticity boundary-value problem for the ITDD in a half-space, we will use radial Somigliana dislocation loops (RSDLs) as virtual surface defects. Single RSDL is shown schematically in Fig. 4. This defect is defined by the following eigenstrain [23]:

$$\varepsilon^{*}_{zr} = \omega r H\left(1-\frac{r}{c}\right)\delta(z), \tag{15}$$

where $\omega$ is the magnitude multiplier of the radial displacement vector of a disclination loop, $c$ is the radius of the loop.

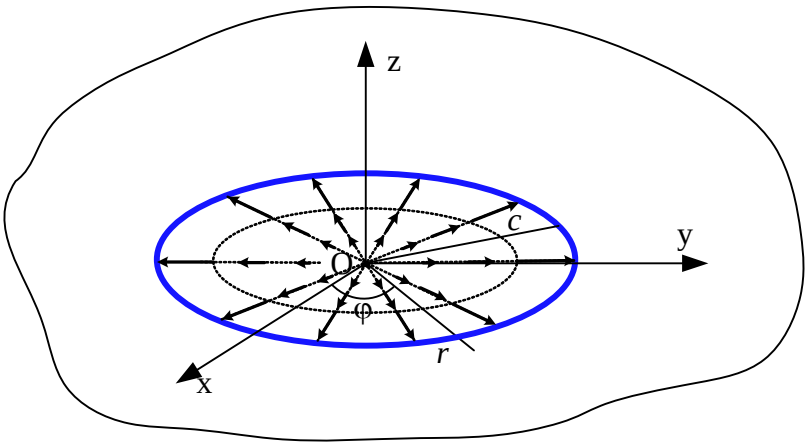


**Fig. 4**. Radial Somigliana dislocation loop (RSDL) with radius $c$ in the infinite elastically isotropic medium

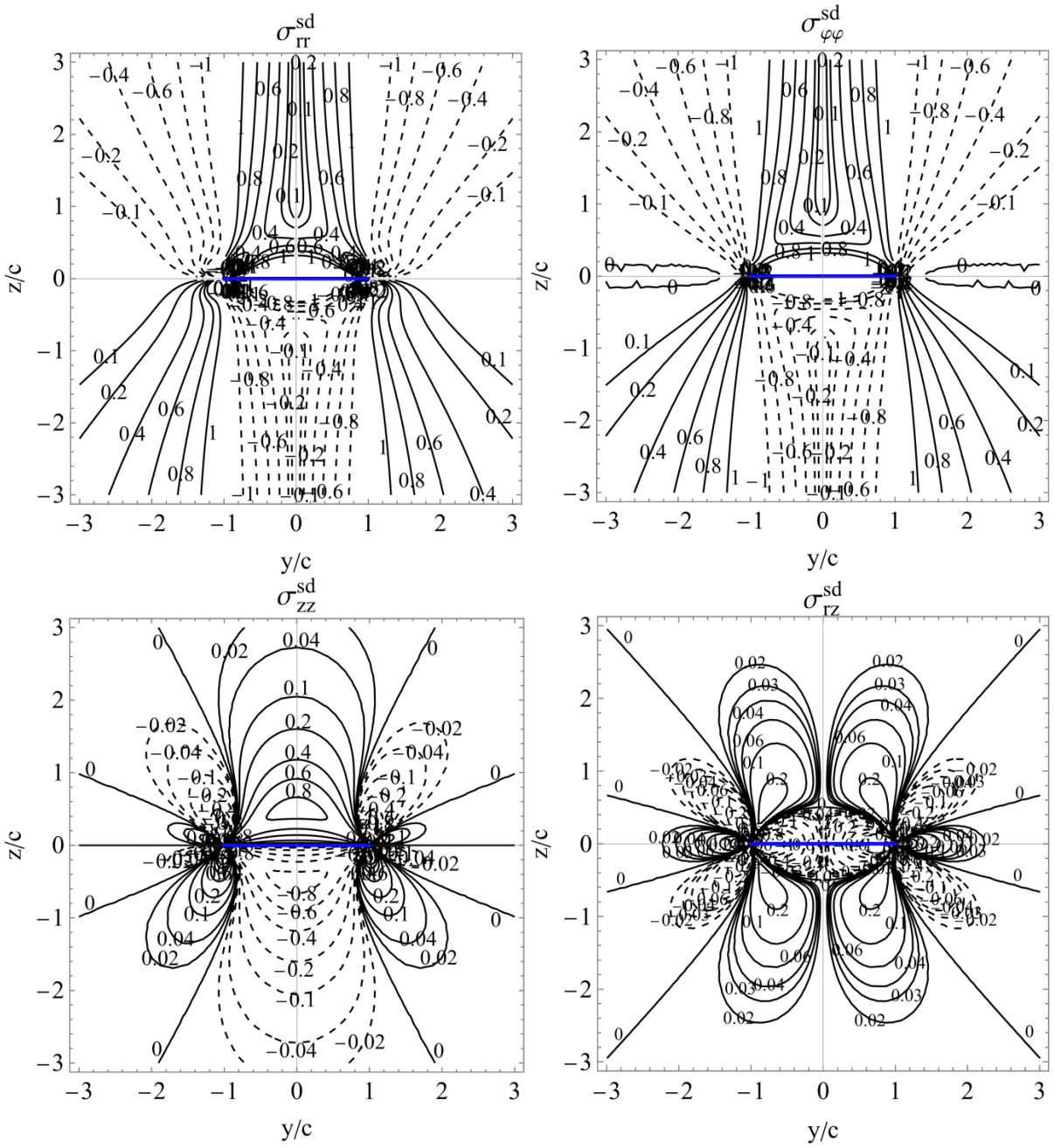


**Fig. 5**. Stress maps in the *zy*-plane for the RSDL with radius *c* located in an infinite elastically isotropic medium. Stresses are given in units of $\frac{G\omega}{2(1-\nu)}$ and the coordinates are normalized to the loop radius *c*

The elastic fields of RSDL in an isotropic elastic medium can be derived from the total displacements $u_i^{\mathrm{sd}}$ found in Ref. [26]

$$u_r^{\mathrm{sd}} = \frac{\omega\ \mathrm{sgn}(z)\, c}{4(1-\nu)}\left[ 2(1-\nu)\ J(2,1;0)\Big|_{\substack{z_0=0\\ a\to c}} - \frac{|z|}{c}\, J(2,1;1)\Big|_{\substack{z_0=0\\ a\to c}} \right], \tag{16a}$$

$$u_\varphi^{\mathrm{sd}} = 0, \tag{16b}$$

$$u_z^{\mathrm{sd}} = \frac{\omega c}{4(1-\nu)}\left[ (2\nu-1) J(2,0;0) - \frac{|z|}{c} J(2,0;1) \right]. \tag{16c}$$

These displacements lead to the following elastic strains $\varepsilon_{ij}^{\mathrm{sd}}$ and stresses $\sigma_{ij}^{\mathrm{sd}}$:

$$\varepsilon_{rr}^{\mathrm{sd}} = \frac{\omega \operatorname{sgn}(z)}{4(1-\nu)}\left[2(1-\nu)J(2,0;1) - 2(1-\nu)\frac{c}{r}J(2,1;0) - \frac{|z|}{c}J(2,0;2) + \frac{|z|}{r}J(2,1;1)\right], \tag{17a}$$

$$\varepsilon_{\varphi\varphi}^{\mathrm{sd}} = \frac{\omega \operatorname{sgn}(z)}{4(1-\nu)}\left[2(1-\nu)\frac{c}{r}J(2,1;0) - \frac{|z|}{r}J(2,1;1)\right], \tag{17b}$$

$$\varepsilon_{zz}^{\mathrm{sd}} = \frac{\omega \operatorname{sgn}(z)}{4(1-\nu)}\left[\frac{|z|}{c}J(2,0;2) - 2\nu J(2,0;1)\right], \tag{17c}$$

$$\varepsilon_{rz}^{\mathrm{sd}} = \frac{\omega}{4(1-\nu)}\left[\frac{|z|}{c}J(2,1;2) - J(2,1;1)\right], \tag{17d}$$

$$\varepsilon_{r\varphi}^{\mathrm{sd}} = \varepsilon_{z\varphi}^{\mathrm{sd}} = 0. \tag{17e,f}$$

$$\sigma_{rr}^{\mathrm{sd}} = \frac{G\omega\ \operatorname{sgn}(z)}{2(1-\nu)}\left[2(\nu-1)\frac{c}{r}J(2,1;0) - \frac{|z|}{c}J(2,0;2) + 2J(2,0;1) + \frac{|z|}{r}J(2,1;1)\right], \tag{18a}$$

$$\sigma_{\varphi\varphi}^{\mathrm{sd}} = \frac{G\omega\ \operatorname{sgn}(z)}{2(1-\nu)}\left[2(1-\nu)\frac{c}{r}J(2,1;0) - \frac{|z|}{r}J(2,1;1) + 2\nu J(2,0;1)\right], \tag{18b}$$

$$\sigma_{zz}^{\mathrm{sd}} = \frac{G\omega}{2(1-\nu)}\frac{z}{c}J(2,0;2), \tag{18c}$$

$$\sigma_{rz}^{\mathrm{sd}} = \frac{G\omega}{2(1-\nu)}\left[\frac{|z|}{c}J(2,1;2) - J(2,1;1)\right], \tag{18d}$$

$$\sigma_{r\varphi}^{\mathrm{sd}} = \sigma_{z\varphi}^{\mathrm{sd}} = 0. \tag{18e, )}$$

The RSDL stress maps were plotted in accordance with Eqs. (18) are given in Fig. 5. An important property of the found stresses is the absence of $\sigma_{zz}$ components at $z$=0. This feature will be used below in the solution of the elasticity boundary-value problem for the ITDD.

## 4. Elastic field of ITDD in the isotropic elastic half-space

**Implementation of the virtual defect technique to the elasticity problem for the ITDD in a half-space.** In our model, shown schematically in Fig. 6, the real ITDD is located at $z = -d$, the mirror ITDD – at $z = +d$, virtual RSDLs are on the free surface with unknown distribution function $f(c)$.

According to Eq. (3) boundary conditions for the stresses of ITDD, that is in the elastic half-space, can be written as:

$$\sigma_{zz}^{\mathrm{hs}}\Big|_{z=0} = 0, \tag{19a}$$

$$\sigma_{zr}^{\mathrm{hs}}\Big|_{z=0} = 0. \tag{19b}$$

We search for the stresses of ITDD in the following representation:

$$\sigma_{ij}^{\mathrm{hs}} = \sigma_{ij} + \sigma_{ij}^{\mathrm{i}}, \tag{20}$$

where $\sigma_{ij}$ are the stresses of the real defect (i.e., ITDD) in infinite elastic space and an additional $\sigma_{ij}^{i}$ term comes from virtual defects. There are two boundary conditions in Eqs. (19); therefore, we consider the additional field as the sum of two members:

$$\sigma_{ij}^{\mathrm{i}} = \sigma_{ij}^{\mathrm{md}} + \sigma_{ij}^{\mathrm{ssd}}, \tag{21}$$

where $\sigma_{ij}^{md}$ is due to virtual dilatation disk of opposite dilatation sign (mirror disk) and $\sigma_{ij}^{ssd}$ is due to RDSLs distributed continuously with radial density $f(c)$ on the free surface $z = 0$ (Fig. 4). Variable $c$ is the radius of a probe loop in the distribution of RDSLs.

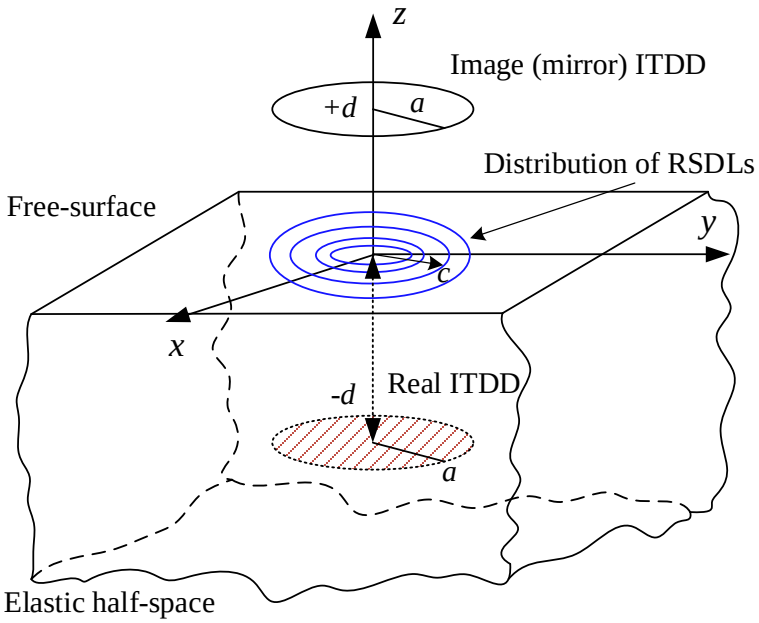


**Fig. 6.** Schematics of defect configuration used in the solution of the elasticity boundary-value problem for real ITDD. Image (mirror) ITDD with opposite signs of dilatation and distribution of surface RSDLs are used as virtual defects

In the framework of the proposed model, boundary conditions become the integral equations with respect to unknown distribution function $f(c)$:

$$\sigma_{zz}\Big|_{z=0} + \sigma_{zz}^{md}\Big|_{z=0} + \int_0^{+\infty} f(c)\,\sigma_{zz}^{sd}(r,c,z)\Big|_{z=0}\,dc = 0, \tag{22a}$$

$$\sigma_{zr}\Big|_{z=0} + \sigma_{zr}^{md}\Big|_{z=0} + \int_0^{+\infty} f(c)\,\sigma_{zr}^{sd}(r,c,z)\Big|_{z=0}\,dc = 0, \tag{22b}$$

where we must take into account that

$$\sigma_{zz}^{md}\Big|_{z=0} = -\sigma_{zz}\Big|_{z=0} = G\frac{(1+\nu)}{(1-\nu)}\frac{b}{a}\int_0^{+\infty} J_1(\kappa)J_0(\kappa\cdot\frac{r}{a})e^{\frac{-d}{a}\kappa}\kappa d\kappa, \tag{23a}$$

$$\sigma_{zz}^{sd}(r,c,z)\Big|_{z=0} = 0, \tag{23b}$$

$$\sigma_{rz}^{md}\Big|_{z=0} = -\sigma_{rz}\Big|_{z=0} = -G\frac{(1+\nu)}{(1-\nu)}\frac{b}{a}\int_0^{+\infty} J_1(\kappa)J_1(\kappa\cdot\frac{r}{a})e^{\frac{-d}{a}\kappa}\kappa d\kappa, \tag{23c}$$

$$\sigma_{rz}^{sd}(r,c,z)\Big|_{z=0} = \frac{-G\omega}{2(1-\nu)}J(2,1;1)\Big|_{\substack{z_0=+0\\z=0}} = \frac{-G\omega}{2(1-\nu)}\int_0^{+\infty} J_2(\kappa)J_1(\kappa\cdot\frac{r}{c})\kappa d\kappa. \tag{23d}$$

After substitution of Eqs. (23) to the boundary conditions given by Eqs. (22) we arrive in a single integral equation for the function $f(c)$:

$$K\int_0^{+\infty} J_1(\kappa)J_1(\kappa\cdot\frac{r}{a})e^{\frac{-d}{a}\kappa}\kappa d\kappa + \int_0^{+\infty} f(c)dc\int_0^{+\infty} J_2(\kappa)J_1(\kappa\cdot\frac{r}{c})\kappa d\kappa = 0, \tag{24}$$

where $K = 4(1+\nu)\dfrac{b}{a\,\omega}$.

The found integral equation can be solved with the help of the pair of Hankel transformations [29]

$$H_\nu(\lambda) = \int_0^{+\infty} J_\nu(\lambda r)\psi(r) r dr\,. \tag{25}$$

$$\psi(r) = \int_0^{+\infty} J_\nu(\lambda r) H_\nu(\lambda)\lambda d\lambda\,. \tag{26}$$

Introducing a new variable $\beta = \kappa / c$ $(\kappa = \beta c,\, d\kappa = c\, d\beta)$ in the second member of Eq. (24) and changing the order of integrals we get:

$$K\int_0^{+\infty} J_1(\kappa) J_1(\kappa\cdot\frac{r}{a}) e^{\frac{-d}{a}\kappa}\kappa d\kappa + \int_0^{+\infty} J_1(\beta r)\beta d\beta \int_0^{+\infty} J_2(\beta c)\, f(c) c^2 dc = 0\,, \tag{27}$$

that can be reduced to:

$$K\int_0^{+\infty} J_1(\kappa) J_1(\kappa\cdot\frac{r}{a}) e^{\frac{-d}{a}\kappa}\kappa d\kappa + \int_0^{+\infty} J_1(\beta r) H_2(\beta)\beta d\beta = 0\,, \tag{28}$$

where $H_2(\beta) = \int_0^{+\infty} J_2(\beta c)\, f(c) c^2 dc$ is Hankel transform of the function $f(c)c$.

Finally, we get the equation:

$$K\int_0^{+\infty} J_1(\kappa\tilde{r}) J_1(\kappa) e^{-\tilde{d}\kappa}\kappa d\kappa + \int_0^{+\infty} J_1(\kappa\tilde{r}) H_2(\kappa) a^{-2}\kappa d\kappa = 0\,. \tag{29}$$

where the designations $\tilde{r} = r / a$ and $\tilde{d} = d / a$ are introduced.

Applying Hankel transformation to both integrals of Eq. (29) we obtain the algebraic equation for unknown $H_2(\kappa)$ and then find:

$$H_2(\kappa) = -K a^2 J_1(\kappa) e^{-\tilde{d}\kappa}\,. \tag{30}$$

**Elastic field of the ITDD in elastic half-space.** Using the result given by Eq. (30) it is possible to write in the integral form displacements, strains, and stresses of RSDL distribution. Finally, this allows us to determine the desired elastic fields of the ITDD in an isotropic half-space.

***ITDD displacements:***

$$u_r^{\text{hs}} = \frac{(1+\nu)b}{2(1-\nu)}\left[ J^{(1)}(1,1;0) - J^{(2)}(1,1;0) + \operatorname{sgn}(z)\left( \frac{2\,|z|}{a} J^{(3)}(1,1;1) - 4(1-\nu) J^{(3)}(1,1;0) \right)\right], \tag{31a}$$

$$u_\varphi^{\text{hs}} = 0\,, \tag{31b}$$

$$u_z^{\text{hs}} = \frac{(1+\nu)b}{2(1-\nu)}\left[ \operatorname{sgn}(z-z_0) J^{(1)}(1,0;0) - \operatorname{sgn}(z-z_0) J^{(2)}(1,0;0) + \frac{2|z|}{a} J^{(3)}(1,0;1) - 2(2\nu-1) J^{(3)}(1,0;0)\right], \tag{31c}$$

where $J^{(1)}(m,n;p) = \int_0^\infty J_m(\kappa) J_n(\kappa\frac{r}{c})\kappa^p e^{-\kappa\xi_1} d\kappa;\ \xi_1 = \dfrac{|z+d|}{c}$,

$$J^{(2)}(m,n;p) = \int_0^\infty J_m(\kappa) J_n(\kappa\frac{r}{c})\kappa^p e^{-\kappa\xi_2} d\kappa;\ \xi_2 = \frac{|z-d|}{c}\,,$$

$$J^{(3)}(m,n;p) = \int_0^\infty J_m(\kappa) J_n(\kappa\frac{r}{c})\kappa^p e^{-\kappa\xi_3} d\kappa;\ \xi_3 = \frac{|z|+d}{c}\,.$$

***ITDD strains:***

$$\varepsilon_{rr}^{\mathrm{hs}}=\frac{(1+\nu)b}{(1-\nu)a}\left[\frac{1}{2}J^{(1)}(1,0;1)-\frac{1}{2}\frac{a}{r}J^{(1)}(1,1;0)-\frac{1}{2}J^{(2)}(1,0;1)+\frac{1}{2}\frac{a}{r}J^{(2)}(1,1;0)\right.$$
$$\left.+\operatorname{sgn}(z)\left(-2(1-\nu)J^{(3)}(1,0;1)+a\frac{2(1-\nu)}{r}J^{(3)}(1,1;0)+\frac{|z|}{a}J^{(3)}(1,0;2)-\frac{|z|}{r}J^{(3)}(1,1;1)\right)\right], \quad (32a)$$

$$\varepsilon_{\varphi\varphi}^{\mathrm{hs}}=\frac{(1+\nu)b}{(1-\nu)a}\left[\frac{a}{2r}J^{(1)}(1,1;0)-\frac{a}{2r}J^{(1)}(1,1;0)+\operatorname{sgn}(z)\left(\frac{|z|}{r}J^{(2)}(1,1;1)-\frac{2(1-\nu)a}{r}J^{(2)}(1,1;0)\right)\right], \quad (32b)$$

$$\varepsilon_{zz}^{\mathrm{hs}}=\frac{(1+\nu)b}{(1-\nu)a}\left[-\frac{1}{2}J^{(1)}(1,0;1)+\frac{1}{2}J^{(2)}(1,0;1)+\operatorname{sgn}(z)\left(2\nu J^{(3)}(1,0;1)-\frac{1}{a}|z|J^{(3)}(1,0;2)\right)\right], \quad (32c)$$

$$\varepsilon_{rz}^{\mathrm{hs}}=\frac{(1+\nu)b}{(1-\nu)a}\left[\frac{1}{2}\operatorname{sgn}(z-z_0)J^{(1)}(1,1;1)-\frac{1}{2}\operatorname{sgn}(z-z_0)J^{(2)}(1,1;1)+J^{(3)}(1,1;1)-\frac{|z|}{a}J^{(3)}(1,1;2)\right], \quad (32d)$$

$$\varepsilon_{r\varphi}^{\mathrm{hs}}=\varepsilon_{\varphi z}^{\mathrm{hs}}=0. \quad (32e,f)$$

***ITDD stresses:***

$$\sigma_{rr}^{\mathrm{hs}}=G\frac{(1+\nu)b}{(1-\nu)}\left[\left(\frac{1}{a}J^{(1)}(1,0;1)-\frac{1}{r}J^{(1)}(1,1;0)\right)-\left(\frac{1}{a}J^{(2)}(1,0;1)-\frac{1}{r}J^{(2)}(1,1;0)\right)+\left(\frac{2|z|}{a^2}\operatorname{sgn}(z)J^{(3)}(1,0;2)\right.\right.$$
$$\left.\left.-\frac{4(\nu-1)}{r}\operatorname{sgn}(z)J^{(3)}(1,1;0)-\frac{4}{a}\operatorname{sgn}(z)J^{(3)}(1,0;1)-\frac{2|z|}{a\,r}\operatorname{sgn}(z)J^{(3)}(1,1;1)\right], \quad (33a)$$

$$\sigma_{\varphi\varphi}^{\mathrm{hs}}=G\frac{(1+\nu)b}{(1-\nu)}\left[\frac{1}{r}J^{(1)}(1,1;0)-\frac{1}{r}J^{(2)}(1,1;0)-\frac{4(1-\nu)\operatorname{sgn}(z)}{r}J^{(3)}(1,1;0)\right.$$
$$\left.+\frac{2|z|}{a\,r}\operatorname{sgn}(z)J^{(3)}(1,1;1)-\frac{4\nu\operatorname{sgn}(z)}{a}J^{(3)}(1,0;1)\right], \quad (33b)$$

$$\sigma_{zz}^{\mathrm{hs}}=G\frac{(1+\nu)b}{(1-\nu)}\left[-\frac{1}{a}J^{(1)}(1,0;1)+\frac{1}{a}J^{(2)}(1,0;1)-\frac{2z}{a^2}J^{(3)}(1,0;2)\right], \quad (33c)$$

$$\sigma_{zr}^{\mathrm{hs}}=\frac{G(1+\nu)b}{(1-\nu)a}\left[-\operatorname{sgn}(z-z_0)J^{(1)}(1,1;1)+\operatorname{sgn}(z-z_0)J^{(2)}(1,1;1)+2J^{(3)}(1,1;1)-\frac{2|z|}{a}J^{(3)}(1,1;2)\right]. \quad (33d)$$

***Hydrostatic stress:***

$$\sigma^{\mathrm{hs}}=\sum\sigma_{ii}^{\mathrm{hs}}=\sigma_{rr}^{\mathrm{hs}}+\sigma_{\phi\phi}^{\mathrm{hs}}+\sigma_{zz}^{\mathrm{hs}}=-4G\operatorname{sgn}(z)\frac{(1+\nu)^2b}{(1-\nu)a}J^{(3)}(1,0;1). \quad (34)$$

The maps of non-zero stress tensor components of the ITDD in a half-space are given in Fig. 7, whereas Fig. 8 presents the plots for hydrostatic stress (trace of the stress tensor) for the ITDD positioned at various distances from the free surface of a half-space.

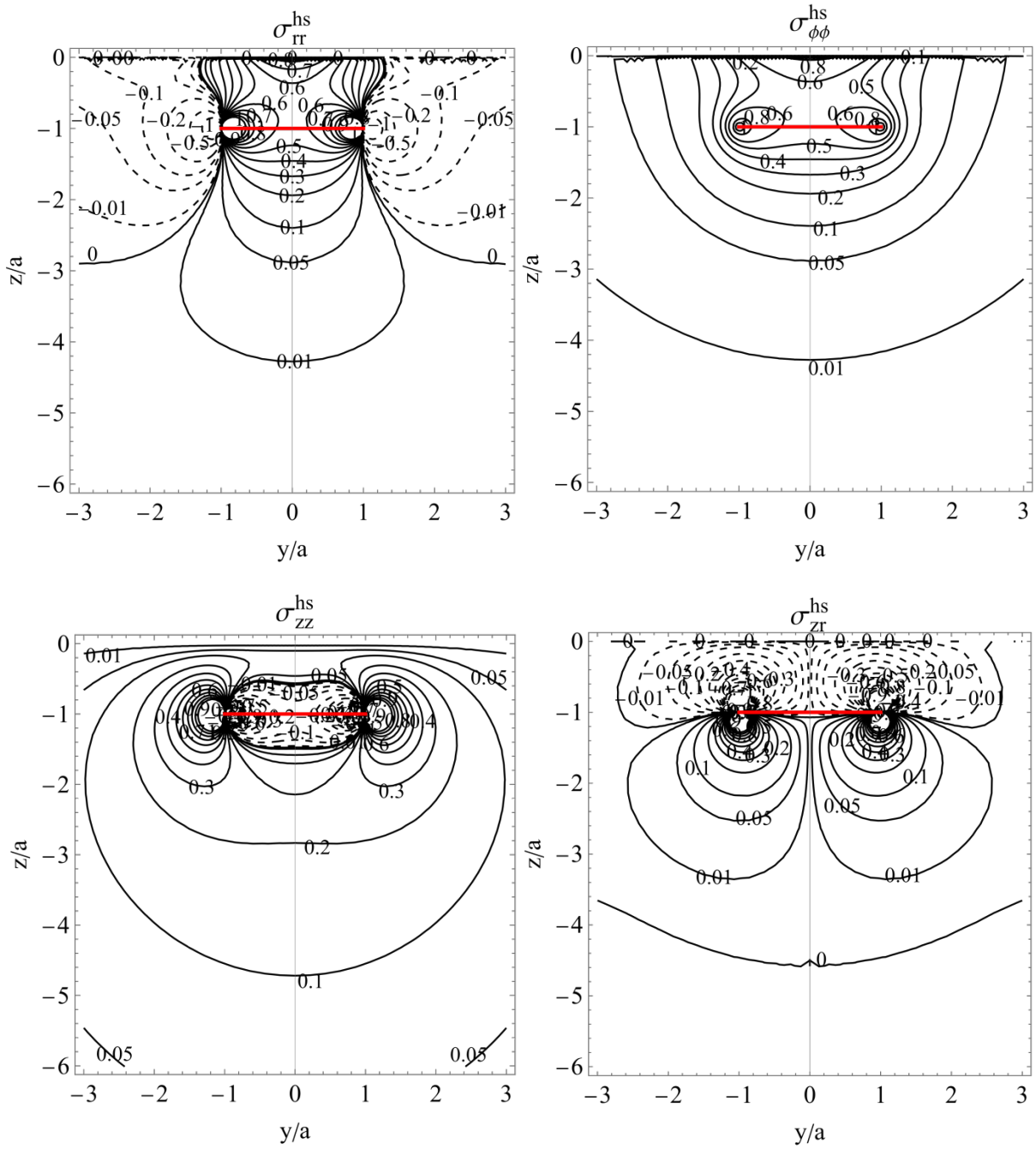


**Fig. 7.** Stress maps in the *zy* - plane for the ITDD, which is in a half-space. The stresses are given in units of $G\frac{(1+\nu)b}{(1-\nu)a}$ and the coordinates are normalized to the disk radius $a$. Parameters used for plots: the ITDD coordinate $z_0$=-$a$, Poisson ratio $\nu$ = 0.234

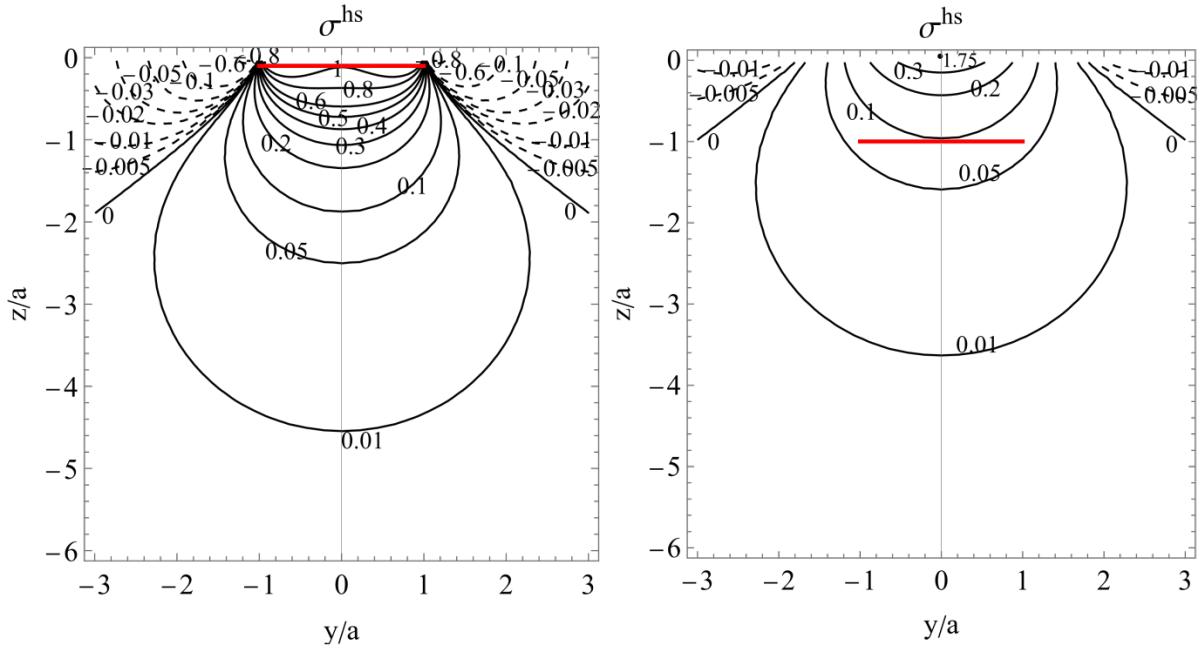


**Fig. 8**. Maps of hydrostatic stress in the *zy* - plane for the ITDD located in elastically isotropic half-space. Stress is given in units of $G\frac{(1+\nu)b}{(1-\nu)a}$ and the coordinates are normalized to the disk radius *a*. Parameters of calculations: ITDD coordinate (a) $z_0$ = - 0.1*a* and (b) $z_0$ = - *a*; Poisson ratio $\nu = 0.234$

## 5. Discussion

In this study, we investigated the elasticity boundary-value problem for infinitesimally thin dilatational disk (ITDD) placed in the vicinity of the free surface of an isotropic half-space. The ITDD was defined by its eigenstrain, see Eq. (1), and the elastic field of ITDD in an infinite elastic medium, see Eqs. (9), (11), and (13), was used as a starting point for the solution. Other important steps of the solution included the introduction of virtual defects: the mirror ITDD with dilatation of opposite sign and surface distribution of radial Somigliana dislocation loops (RSDLs), see Fig. 6. With the aid of chosen virtual defects, the boundary conditions on the free surface could be transformed to a single integral equation, see Eq. (24), with respect to the distribution function $f(c)$ of RSDLs with a variable radius $c$. Then, the Hankel transform of the product $f(c)c$ was found in the concise form, see Eq. (30), which allowed us to get final formulas for the elastic field of the ITDD in the isotropic half-space, see Eqs. (31) to (34). These formulas were written in terms of Lipschitz-Hankel integrals (defined by Eq. (10)), which are easily represented via elliptic functions. The last fact ensured fast numerical manipulation and plotting the maps of ITDD stresses.

It was found that the boundary conditions significantly change the distribution of the stress field of the ITDD in the half-space, see Fig. 7, compared to the case of the infinite medium, see Fig. 3. Due to the presence of a free surface, the symmetry of the elastic field about the plane containing ITDD is broken. Obviously, Eqs. (31) to (34) establish the dependence of the elastic field on the position of the ITDD relative to the free surface, i.e., on the depth *d*. As the ITDD approaches the free surface, the elastic field becomes localized and demonstrates larger gradients. This may affect materials properties, more specifically electronic and optoelectronic properties of semiconductors, as was noted in the Introduction Section.

Expression (34) reflects the fact that in a half-space there is the appearance of the ITDD hydrostatic stress. This is different from the case of the ITDD in an infinite elastically

isotropic medium, where the hydrostatic stress is zero. The examples of hydrostatic stress $\sigma^{hs}$ maps are given in Fig. 8. The important feature that is seen in the plots is the localization of $\sigma^{hs}$ in the layer between ITDD and free surface. When ITDD approaches the surface the level of hydrostatic stress increases. In general, the occurrence of hydrostatic stress is caused by the breaking of the symmetry of the medium by the presence of the free surface. As it was discussed, e.g., in Ref. [10], the modification of stressor elastic field leading to the hydrostatic stress and volumetric elastic strain strongly influence the position of the semiconductor valence band and bandgap. We plan to investigate this effect in more detail for stressors of different shapes in our ongoing study.

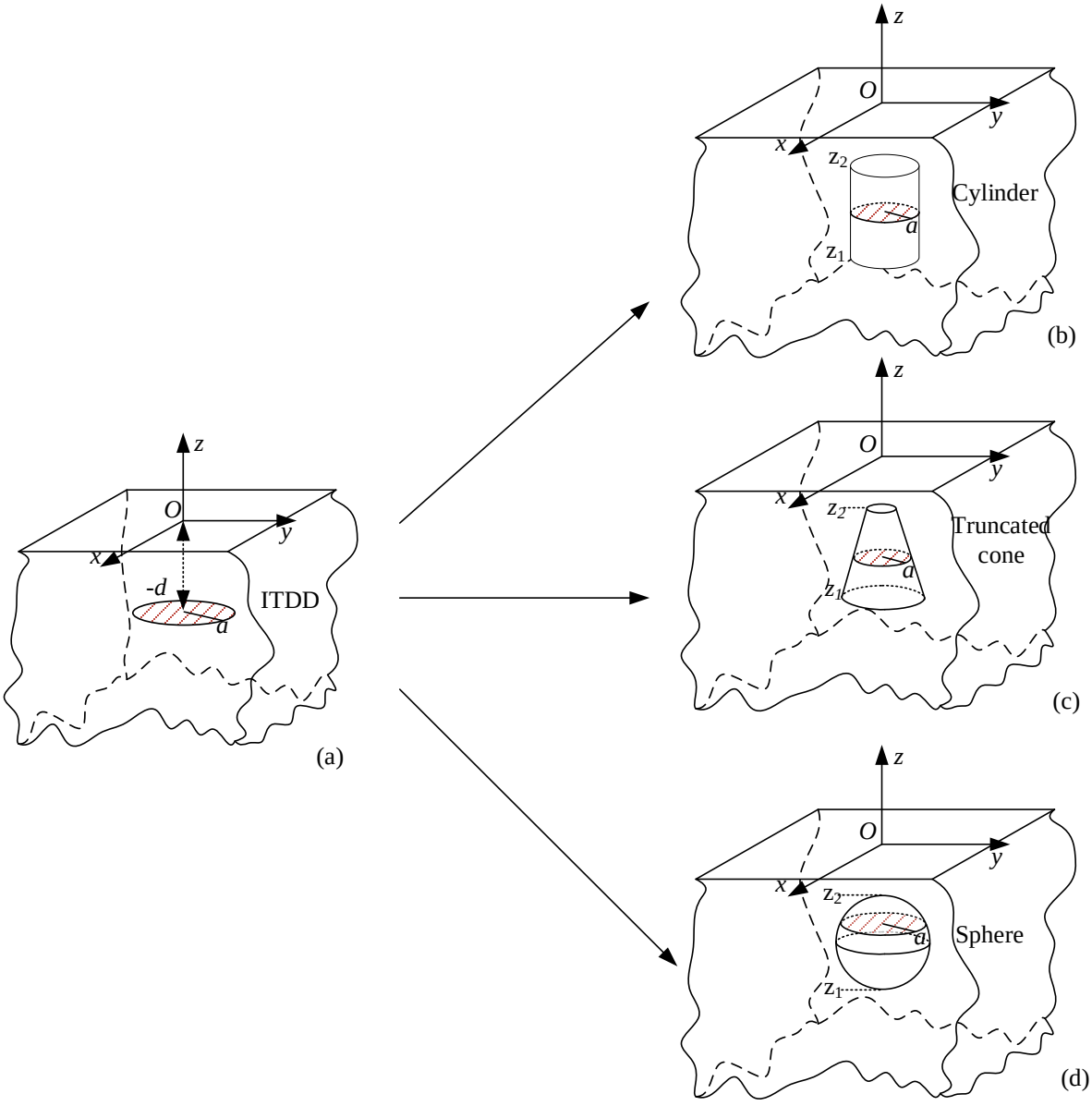


**Fig. 9**. A single infinitesimally thin dilatational disk (ITDD) (a) and axisymmetric dilatational inclusions composed of ITDDs: a cylinder (b), a truncated cone (c), a sphere (d)

Exploring the obtained results, we propose to model stressors with cylindrical symmetry with the help of sets of coaxial ITDDs, see schematics in Fig. 9. By doing so, we can utilize the found for the ITDD solution to determine the elastic field in half-space for dilatational inclusions with the following shapes: a cylinder, a solid cone, a sphere, an ellipsoid, etc. The

elastic fields of such inclusions can be derived from the elastic field of the ITDD according to simple integral formulas (for three cases considered in Fig. 9):

$$\sigma_{ij}^{\mathrm{cl}} = \int_{z_1}^{z_2} \sigma_{ij}^{\mathrm{ssd}}(z)\frac{\varepsilon_\Delta}{b}dz, \tag{38a}$$

$$\sigma_{ij}^{\mathrm{tc}} = \int_{z_1}^{z_2} \sigma_{ij}^{\mathrm{ssd}}(z,a(z))\frac{\varepsilon_\Delta}{b}dz, \tag{38b}$$

$$\sigma_{ij}^{\mathrm{sp}} = \int_{z_1}^{z_2} \sigma_{ij}^{\mathrm{ssd}}(z,a(z))\frac{\varepsilon_\Delta}{b}dz, \tag{38c}$$

where $\sigma_{ij}^{\mathrm{cl}}, \sigma_{ij}^{\mathrm{tc}}, \sigma_{ij}^{\mathrm{sp}}$ are the stresses of dilatating cylinder, truncated cone, and sphere, respectively; $\frac{\varepsilon_\Delta}{b}$ is linear (axial) density in ITDD distributions with $\varepsilon_\Delta$ designating $\frac{1}{3}$ of the volumetric strain of the dilatating inclusion. In Eqs. (38b,c), the radius *a* is variable, which depends on the axial variable *z* (*a* = *a*(*z*)), but in Eq. (38a) *a* is constant.

## 6. Summary and conclusions

We have found an analytical solution to the elasticity boundary-value problem for infinitesimally thin dilatational disk (ITDD) placed in the vicinity of the free surface of elastically isotropic half-space. The ITDD displacements, strains, and stresses have been determined in a close and concise form. The results obtained have demonstrated that the boundary conditions significantly affect the ITDD elastic field in the case of a half-space compared to the case of an infinite medium. An important feature of the ITDD elastic field in semi-infinite medium concerns the emergence of hydrostatic stress and volumetric strain which are not peculiar to dilatational defects in an infinite elastically isotropic medium. This property needs to be taken into account when analyzing the stressor effect on various physical and mechanical materials characteristics including those for semiconductors where strain-related effects can be essential. Finally, we have outlined the use of the obtained results for the elastic analysis of finite volume cylindrically symmetric dilatational inclusions.

## References

[1] Freund LB, Suresh S. *Thin film materials: stress, defect formation and surface evolution*. Cambridge, UK: Cambridge University Press; 2003.

[2] Smirnov AM, Young EC, Bougrov VE, Speck JS, Romanov AE. Stress relaxation in semipolar and nonpolar III-nitride heterostructures by formation of misfit dislocations of various origin. *Journal of Applied Physics*. 2019;126(24): 245104.

[3] Gutkin MY, Kolesnikova AL, Mikheev DS, Romanov AE. Misfit stresses and their relaxation by misfit dislocation loops in core-shell nanoparticles with truncated spherical cores. *European Journal of Mechanics A/Solids*. 2020;81: 103967.

[4] Chernakov AP, Kolesnikova AL, Gutkin MY, Romanov AE. Periodic array of misfit dislocation loops and stress relaxation in core-shell nanowires. *International Journal of Engineering Science*. 2020;156: 103367.

[5] Kossoy A, Frenkel AI, Wang Q, Wachtel E, Lubomirsky I. Local structure and strain-induced distortion in Ce0.8Gd0.2O1.9. *Advanced Materials.* 2010;22(14): 1659-1662.

[6] Zhang W, Cheng F, Huang J, Yuan H, Wang Q. Investigation of uniaxial strain in twisted few-layer MoS2. *Physics Letters A*. 2021;418: 127709.

[7] Chibueze TC, Ekuma CE, Raji AT, Ezema FI, Okoye CMI. Tetragonal and uniaxial strains in pristine and doped half-Heusler AuMnSn alloy. *Journal of Alloys and Compounds*. 2020;484: 156186.

[8] O'Hare A, Kusmartsev FV, Kugel KI. Stable "flat" form of two-dimensional crystals: could graphene, silicene, germanene be minigap semiconductors. *Nano Letter*. 2012;12(2): 1045-1052.
[9] Bir GL, Pikus GE. *Symmetry and deformation effects in semiconductors*. New York: John Wiley & Sons; 1974.
[10] Romanov AE, Waltereit P, Speck JS. Buried stressors in nitride semiconductors: Influence on electronic properties. *Journal of Applied Physics*. 2005;97(4): 043708.
[11] Kuo CP, Vong SK, Cohen RM, Stringfellow GB. Effect of mismatch strain on band gap in III-V semiconductors. *Journal of Applied Physics*. 1985;57(12): 5428-5432.
[12] Tilley R. *Defects in solids*. New York: John Wiley & Sons, INC; 2008.
[13] Kolesnikova AL, Gutkin MY, Romanov AE. Elastic models of defects in 3D and 2D crystals. *Reviews on Advanced Materials Science*. 2017;51: 130-148.
[14] Chou YT. The energy of circular dislocation loops in thin plates. *Acta Metallurgica*. 1963;11(8): 829-834.
[15] Xia R, Wu W, Wu R. Elastic field due to dislocation loops in isotropic multilayer system. *Journal of Materials Scienc*e. 2016;51: 2942-2957.
[16] Romanov AE, Beltz GE, Fischer WT. Elastic fields of quantum dots in subsurface layers. *Journal of Applied Physics*. 2001;89(8): 4523-4531.
[17] Melezhik E, Korotchenkov O. Elastic fields of quantum dots in semi-infinite matrices: green's function analytical analysis. *Journal of Applied Physics*. 2009;105(2): 023525.
[18] Liu S, Jin X, Wang Z, Keer LM, Wang Q. Analytical solution for elastic fields caused by eigenstrains in a half-space and numerical implementation based on FFT. *International Journal of Plasticity*. 2012;35: 135-154.
[19] Jasiuk I, Sheng PY, Tsuchida E. A spherical inclusion in an elastic half-space under shear. *Journal of Applied Mechanic*. 1997;64(3): 471-479.
[20] Kolesnikova AL, Gutkin MY, Romanov AE. Analytical elastic models of finite cylindrical and truncated spherical inclusions. *International Journal of Solids and Structure*. 2018;143: 59-72.
[21] Timoshenko S, Goodier JN. *Theory of elasticity*. New York: McGraw-Hill book company; 1951
[22] Hirth JP, Lothe J. *Theory of dislocations*. New York: John Wiley & Sons; 1982.
[23] Kolesnikova AL, Romanov AE. Virtual circular dislocation-disclination loop technique in boundary value problems in the theory of defects. *Journal of Applied Mechanic*. 2004;71(3): 409-417.
[24] Louat N, Sadananda K. Some consequences of the elastic interaction of particles and free surfaces. *Philosophical Magazine A*. 1991;64(1): 213-221.
[25] Dundurs J, Salamon NJ. Circular prismatic dislocation loop in two-phase material. *Journal of Physics C: Solid State*. 1972;50(1): 125-133.
[26] Kolesnikova AL, Romanov AE. *Circular dislocation-disclination loops and their application to boundary problem solution in the theory of defects*. Leningrad: Ioffe Physical-Technical Institute; 1986. (In Russian)
[27] Kolesnikova AL, Soroka RM, Romanov AE. Defects in the elastic continuum: classification, fields and physical analogies. *Materials Physics and Mechanics*. 2013;17(1): 71-79.
[28] Mura T. *Micromechanics of defects in solids*. Dordrcht: Martinus Nijhoff Publishers; 1987.
[29] Debnath L, Bhatta D. *Integral transforms and their applications*. Boca Raton: Taylor & Francis Group, LLC; 2007.

## THE AUTHORS

**Nguyen Van T.**
e-mail: nguyenvantuyendhsd@gmail.com
ORCID: 0000-0002-7996-1538

**Kolesnikova A.L.**
e-mail: anna.kolesnikova.physics@gmail.com
ORCID: 0000-0003-4116-4821

**Romanov A.E.**
e-mail: alexey.romanov@niuitmo.ru
ORCID: 0000-0003-3738-408X